PLOS ONE

RESEARCH ARTICLE

Involvement of GLUT1 and GLUT3 in the growth of canine melanoma cells

Yoko Suwabe[1], Rei Nakano[1,2], Shinichi Namba[1], Naoya Yachiku[1], Manami Kuji[1], Mana Sugimura[1], Nanako Kitanaka[1], Taku Kitanaka[1], Tadayoshi Konno[3], Hiroshi Sugiya[3], Tomohiro Nakayama[1] *

1 Laboratories of Veterinary Radiotherapy, Nihon University College of Bioresource Sciences, Kameino, Fujisawa, Kanagawa, Japan, 2 Laboratory for Cellular Function Conversion Technology, RIKEN Center for Integrative Medical Sciences, Suehiro-cho, Tsurumi, Yokohama, Kanagawa, Japan, 3 Laboratories of Veterinary Biochemistry, Nihon University College of Bioresource Sciences, Kameino, Fujisawa, Kanagawa, Japan

☯ These authors contributed equally to this work.
* nakayama.tomohiro80@nihon-u.ac.jp

Abstract

The rate of glucose uptake dramatically increases in cancer cells even in the presence of oxygen and fully functioning mitochondria. Cancer cells produce ATP by glycolysis rather than oxidative phosphorylation under aerobic conditions, a process termed as the "Warburg effect." In the present study, we treated canine melanoma cells with the glucose analog 2-deoxy-D-glucose (2-DG) and investigated its effect on cell growth. 2-DG attenuated cell growth in a time- and dose-dependent manner. Cell growth was also inhibited following treatment with the glucose transporter (GLUT) inhibitor WZB-117. The treatment of 2-DG and WZB-117 attenuated the glucose consumption, lactate secretion and glucose uptake of the cells. The mRNA expression of the subtypes of GLUT was examined and *GLUT1* and *GLUT3* were found to be expressed in melanoma cells. The growth, glucose consumption and lactate secretion of melanoma cells transfected with siRNAs of specific for *GLUT1* and *GLUT3* was suppressed. These findings suggest that glucose uptake via GLUT1 and GLUT3 plays a crucial role for the growth of canine melanoma cells.

Introduction

Glucose is a main source of energy and carbon for mammalian cells. It is taken up by the cells via glucose transporters (GLUTs) and metabolized to pyruvate in the cytosol via glycolysis. In normal cells, glycolysis-derived pyruvate is predominantly imported into the mitochondrial matrix where it is oxidized to acetyl coenzyme A (CoA) by the pyruvate dehydrogenase complex. Acetyl CoA is subsequently incorporated into the tricarboxylic acid cycle and undergoes oxidative phosphorylation. However, the glucose metabolism of cancer cells is different from that of normal cells. Cancer cells show increased glucose uptake and glycolysis. Following glycolysis, most pyruvate is converted to lactate in the cytoplasm by the action of lactate dehydrogenase and is secreted. These alterations are evident even in the presence of oxygen to support

mitochondrial respiration. This metabolic phenomenon is termed as aerobic glycolysis or the "Warburg effect" [1–3].

The transport of glucose across the plasma membrane is considered as a key rate-limiting step for glucose metabolism [4–7]. Two distinct transporter families are responsible for transporting glucose into the cell, namely, the sodium-coupled glucose co-transporter (SGLT) and the facilitative GLUT proteins. SGLTs are secondary active transporters that drive the transport of glucose and galactose using the sodium gradient across the cell membrane. In contrast, GLUTs are passive transporters involved in the transport of hexoses such as glucose and other substrates using either a chemical or an electrochemical gradient [4, 6].

There are 14 members of the mammalian GLUT family that are subdivided into three classes based on their protein sequences and structural similarities. Class I comprises GLUT1, GLUT2, GLUT3, GLUT4, and GLUT14, and class II is composed of GLUT5, GLUT7, GLUT9, and GLUT11. Class III transporters include GLUT6, GLUT8, GLUT10, GLUT12, and GLUT13 [6, 7]. Class I GLUT1-GLUT4 are the most studied and established members known for their role in glucose transport in various tissues and cell types [5, 6].

The upregulation in the expression of class I GLUTs has been demonstrated in different cancers [8–11], whereas class II and III GLUTs are not well studied. In human malignant melanoma, the expression of class I GLUTs such as GLUT1 and GLUT3 has been reported to be upregulated and correlated with clinical stages [12, 13]. Additionally, the expression of GLUT1 may predict hypoxia and glycolysis in the tumor tissue as well as the patient outcome [13]. These findings suggest that GLUTs may serve as promising therapeutic targets for melanoma treatment.

Oral malignant melanoma is a naturally occurring cancer in dogs [14]. The canine melanoma is, in general, aggressive, extremely metastatic, and highly associated with poor prognosis. Given its tendency to behave in a biologically aggressive manner similar to that observed in human melanoma, canine melanoma has been considered as a suitable disease model of human cancers [15–17].

In the present study, we investigated the effect of glucose metabolism on the growth of canine melanoma cells. We demonstrated that the suppression of glucose metabolism resulted in the inhibition of cell growth and that class I GLUT subtypes GLUT1 and GLUT3 were involved in the growth of canine melanoma cells.

Materials and methods

Materials

Canine melanoma cells (MCM-N1 cell line; 13-year-old male dog; chromosome number, 2n = 74) were purchased from DS Pharma Biomedical Co., Ltd. (Osaka, Japan). Canine melanoma cell lines (KMeC and CMec-1 [18–20]) were kindly provided by Dr. Takayuki Nakagawa (Laboratory of Veterinary Surgery, Graduate School of Agricultural and Life Sciences, The University of Tokyo). Lipofectamine 2000 and TRIzol were obtained from Life Technologies Co. (Carlsbad, CA). PrimeScript RT Master Mix and Ex Taq were supplied by TaKaRa Bio Inc. (Shiga, Japan). Rabbit monoclonal anti-GLUT1 (EPR3915) and anti-GLUT3 (EPR10508 (N)) antibodies were obtained from Abcam (Cambridge, UK), and mouse monoclonal anti-mouse β-actin antibody (AC74) and GLUT1, GLUT3, and scramble small-interfering RNAs (siRNAs) were procured from Sigma-Aldrich Inc. (St Louis, MO). Horseradish peroxidase (HRP)-conjugated anti-rabbit IgG and anti-mouse IgG antibodies, ECL Western Blotting Analysis System, and ImageQuant LAS 4000 mini were supplied by GE Healthcare (Piscataway, NJ). Mini-PROTEAN TGX gel and polyvinylidene difluoride (PVDF) membranes were obtained from Bio-Rad (Hercules, CA), and Block Ace and complete mini EDTA-free protease

inhibitor mixture were purchased from Roche (Mannheim, Germany). The Dulbecco's modified Eagle medium with 1 g/L glucose (DMEM-LG), phenylmethanesulfonyl fluoride (PMSF), sodium fluoride, and 4-(2-hydroxyethyl)-1-piperazineethanesulfonic acid (HEPES) were obtained from Wako Pure Chemical Industries, Ltd. (Osaka, Japan), and 3-(4,5-dimethyl-2-thiazolyl)-2,5-diphenyl-2H-tetrazolium bromide (MTT) assay reagent, glucose assay kit-WST, lactate assay kit-WST from Dojindo (Tokyo, Japan). 2-(N-(7-Nitrobenz-2-oxa-1,3-dia-zol-4-yl)Amino)-2-Deoxyglucose (2-NBDG) was purchased from Peptide institute Inc (Osaka, Japan). StatMate IV was purchased from ATMS (Tokyo, Japan).

Cell culture

Canine melanoma cells were maintained in static cultures in DMEM-LG supplemented with 10% fetal bovine serum (FBS) in an incubator with 5% CO_2 at 37˚C. The medium was replaced with fresh medium once a week [21]. After reaching 90%–95% confluency, the cells were harvested with 0.25% trypsin-ethylenediaminetetraacetic acid (EDTA) and suspended in the CELLBANKER 1 plus medium at a density of 2×10^6 cells/500 μL for cryopreservation. Cell suspensions (500 μL) were placed in sterilized serum tubes, which were stored in a freezing vessel (BICELL) and cryopreserved at −80˚C. Before experiments, the tubes were removed from the BICELL vessel and immersed in a water bath at 37˚C. Thawed cell suspensions were transferred into centrifuge tubes containing DMEM-LG with 10% FBS and centrifuged at 300 $\times g$ for 3 min. Cell pellets obtained were resuspended in DMEM-LG with 10% FBS and transferred into 75-cm^2 culture flasks. Static culture was then carried out under the same condition as prior to cryopreservation. Cells were harvested using 0.25% trypsin-EDTA once they reached approximately 90% confluency. The collected cells were seeded at a density of 1×10^6/75-cm^2 culture flask.

MTT assay

Cells were seeded at a density of 3,000 cells/200 μL in each well of a 96-well plate. MTT assay reagent was dissolved in phosphate-buffered saline (PBS) at a concentration of 5 mg/mL, and 20 μL of the reagent was incubated with cells for 1 h in an incubator with 5% CO_2 at 37˚C. Following incubation, PBS (100 μL) was added to each well. After 1 min, the supernatant was discarded and the MTT formazan crystals were dissolved in 200 μL of 0.04 M hydrochloric acid (HCl) in 2-propanol. The optimal density (O.D.) was detected by a microplate reader (Fluoroskan Ascent FL, Thermo Fisher Scientific K.K., Kanagawa, Japan) at 570-nm wavelength.

Glucose and lactate assay

Cells were seeded at a density of 3×10^5 cells/mL in each well of a 6-well plate. The cells were stimulated with 5 mM 2-deoxy-D-glucose (2-DG) or 60 μM WZB-117 for 72 h and culture supernatants were collected. To measure culture supernatant glucose concentrations, we used an assay kit according to the kit instructions.

2-NBDG uptake assay

Cells were seeded at a density of 3×10^5 cells/mL in 35-mm glass-base dish. The cells were stimulated with 5 mM 2-deoxy-D-glucose (2-DG) or 60 μM WZB-117 for 24 h. 2-NBDG was dissolved in phosphate-buffered saline (PBS) with 10% FBS at a concentration of 50 μM, and 1 mL of the 2-NBDG reagent was incubated with the cells for 30 min in an incubator with 5% CO_2 at 37˚C. Following incubation, the cells were washed with PBS and fixed with 1 mL of 4%

PFA in PBS to each well for 15 min. The fluorescence signal was visualized using a confocal laser scanning microscope (LSM-510; Carl Zeiss AG, Oberkochen, Germany).

Real-Time Polymerase Chain Reaction (RT-PCR)

Total RNA was extracted from canine melanoma cells using the TRIzol® reagent (Life Technologies Co.) according to the manufacturer's instructions. RNA concentration was spectrophotometrically measured by reading the absorbance at 260 nm/280 nm. First-strand cDNA synthesis was carried out using 500 ng of the total RNA and the PrimeScript RT Master Mix (TaKaRa Bio Inc., Shiga, Japan). PCR was performed using 2 μL of first-strand cDNA in a 10-μL total reaction volume with primers specific for GLUT1, GLUT2, GLUT3, and GLUT4 (Table 1) and Ex Taq. PCR was conducted on an iCycler (Bio-Rad, Hercules, CA) as previously reported [18–29]. The thermal cycler was programmed for initial denaturation at 94˚C for 2 min, followed by 25 cycles of denaturation at 94˚C for 30 s, primer annealing at 55˚C for 30 s, and primer extension at 72˚C for 30 s. PCR products were separated using 2% agarose gel electrophoresis, stained with ethidium bromide, and visualized under UV light. The amplification of TATA box-binding protein (TBP) from the same amount of cDNA was applied as an endogenous control.

Western blotting

Western blotting was performed as per methods reported previously [21–32]. The melanoma cells were lysed using a lysis buffer containing 20 mM HEPES, 1 mM PMSF, 10 mM sodium fluoride, and a complete mini EDTA-free protease inhibitor cocktail at pH 7.4. Protein concentrations were adjusted using the Bradford method [33]. Extracted proteins were boiled at 95˚C for 5 min in a sodium dodecyl sulfate (SDS) buffer. Samples were loaded into separate lanes of 7.5% or 12% Mini-PROTEAN TGX gels and electrophoretically separated. Separated proteins were transferred onto PVDF membranes, treated with Block Ace for 50 min at room temperature, and incubated with primary antibodies (GLUT1 [1:1000], GLUT3 [1:1000], and β-actin [1:10000]) for 120 min at room temperature. After washing, the membranes were incubated with an HRP-conjugated anti-rabbit or anti-mouse IgG antibody (1:10000) for 90 min at room temperature. Immunoreactivity was detected using ECL Western Blotting Analysis System. Chemiluminescent signals of the membranes were measured using the ImageQuant LAS 4000 mini.

Transfection of siRNA

The siRNA transfection was performed as per previously described methods with some modifications [24, 27–32]. Canine melanoma cells seeded at a density of 1×10^5 cells/35-mm dish

Table 1. Primers used for RT-PCR.

Gene Name	GenBank ID	Primer sequences	size (bp)
SLC2A1	NM_001159326.1	F: 5′– AGCTGCCATTGCTGTTGCTG –3′	115
(GLUT1)		R: 5′– CACGGTGAAGATGATGAAGACGTA –3′	
SLC2A2	XM_005639915.1	F: 5′–TGTGTGTGCCATCTTCATGTCC–3′	149
(GLUT2)		R: 5′–AGAACTCTGCCACCATGAACCA–3′	
SLC2A3	NM_001003308.1	F: 5′–CTTCAGATCGCGCAGCTACC–3′	118
(GLUT3)		R: 5′–TGCATCTTTGAAGATTCCTGTTGAG–3′	
SLC2A4	NM_001159327.1	F: 5′–GCTTCTGCAACTGGACAAGCAA–3′	178
(GLUT4)		R: 5′–AAGTCAGCCGAGATCTGGTCAA–3′	
TBP	XM_863452	F: 5′–ACTGTTGGTGGGTCAGCACAAG–3′	184
		R: 5′–ATGGTGTGTACGGGAGCCAAG–3′	

https://doi.org/10.1371/journal.pone.0243859.t001

Table 2. Sequences for siRNA transfection.

Gene Name	Gene bank ID	siRNA sequences
SLC2A1 (GLUT1)	NM_001159326.1	GCUGUCUUCUAUUACUCCA
SLC2A3 (GLUT3)	NM_001003308.1	GCUGUUUGUUCCAUCCUUA

https://doi.org/10.1371/journal.pone.0243859.t002

or 5×10^5 cells/90-mm dish were transfected with Opti-MEM containing 5 μL/mL Lipofecta-mine 2000 and 100 nM GLUT1, GLUT3, or scramble siRNA for 6 h. After transfection, the medium was changed to DMEM-LG containing 10% FBS, and the cultures were maintained in an incubator with 5% CO_2 at 37°C for 5 days. The siRNA sequences that were used have been shown in Table 2. The efficiency of siRNA transfection was determined by western blotting.

Statistical analysis

The data from experiments are presented as mean ± standard error of means. Statistical analysis was performed using StatMate IV. The data from the time course study were analyzed using two-way analysis of variance, and the data from other experiments for multiple comparison and paired comparison were analyzed using one-way analysis of variance and paired t test, respectively.

Results

Effect of 2-deoxy-D-glucose on the growth of canine melanoma cells

We first examined the contribution of glucose metabolism to the growth of canine melanoma cells using 2-deoxy-D-glucose (2-DG), a synthetic glucose analog. 2-DG is frequently used as an inhibitor of glucose metabolism, including glycolysis [34–39]. The treatment with 5 mM 2-DG for 3 days resulted in a significant decrease in the growth of cells (Fig 1A). The growth of the cells was inhibited after treatment with various concentrations of 2-DG (0 to 20 mM) for 3 days in a dose-dependent manner (Fig 1B). Glucose consumption and lactate secretion of the cells were attenuated after treatment with 5 mM 2-DG for 3 days (Fig 1C and 1D). As shown in Fig 1E, the 2-DG treatment also attenuated glucose uptake. We observed that the effect of 2-DG on the cellular viability, glucose consumption, lactate secretion and glucose uptake was conserved in several canine melanoma cell lines (S1, S2 and S5 Figs). These results suggest that melanoma cells rely on glucose metabolism for their growth.

Effect of a GLUT inhibitor on the growth of canine melanoma cells

The production of ATP by glycolysis under aerobic conditions (Warburg effect) is important for the growth of several types of cancer cells. Glucose transport across the cell membrane via GLUTs is considered as a rate-limiting step for glycolysis. Thus, we examined the effect of the GLUT inhibitor WZB-117 on the growth of melanoma cells. The cells were incubated with 60 μM WZB-117 for 3 days that led to a significant attenuation of their growth (Fig 2A). The treatment of cells with 0 to 60 μM WZB-117 resulted in a significant decrease in their growth in a dose-dependent manner (Fig 2B). When the cells were treated with 60 μM WZB-117 for 3 days, glucose consumption and lactate secretion of the cells were significantly attenuated (Fig 2C and 2D). We also observed that the WZB-117 treatment also attenuated glucose uptake (Fig 2E). As shown in S3, S4 and S5 Figs, WZB-117 showed the significant decrease in the cellular viability, glucose consumption, lactate secretion and glucose uptake of several canine melanoma cell lines.
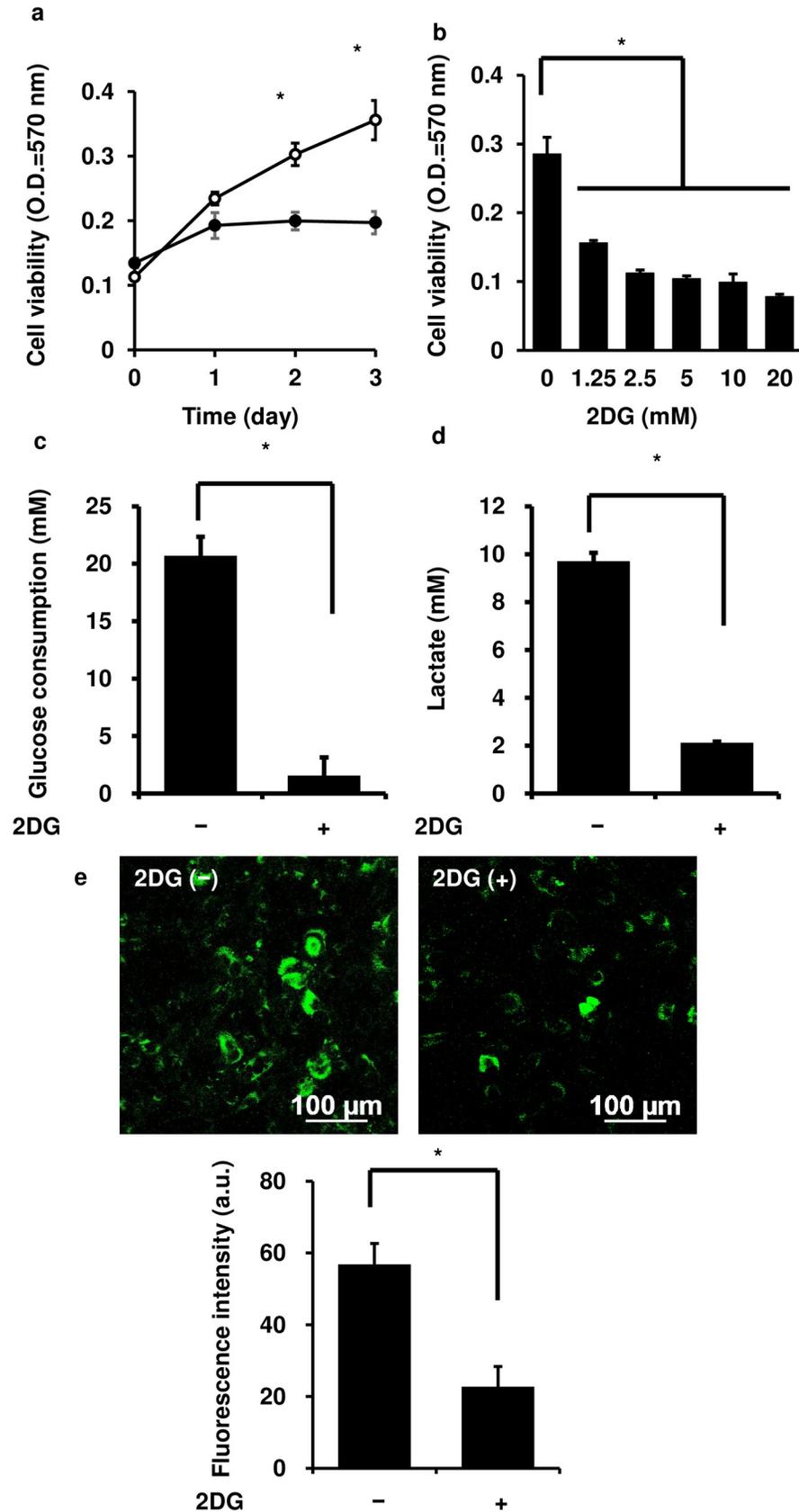
Fig 1. Effect of 2-deoxy-D-glucose on the growth of canine melanoma cells. (a) Time-dependent changes in the growth of canine melanoma cells with (closed circle) or without (open circle) 2-deoxy-D-glucose (2-DG) treatment. The cells were incubated with 5 mM 2-DG for 3 days, and their growth was found to be significantly attenuated. (b) Dose-dependent effect of 2-DG on the growth of canine melanoma cells. The cells were incubated with 0 to 20 mM 2-DG, which attenuated their growth in a dose-dependent manner. (c) The effect of 2-DG on glucose consumption of canine melanoma cells. The cells were incubated with 5 mM 2-DG for 3 days, and glucose consumption was found to be significantly attenuated. (d) The effect of 2-DG on lactate secretion of canine melanoma cells. The cells were incubated with 5 mM 2-DG for 3 days, and lactate secretion was found to be significantly attenuated. (e) The effect of 2-DG on glucose uptake of canine melanoma cells. The cells were incubated with 5 mM 2-DG for 3 days, and glucose uptake was found to be significantly attenuated. Results are shown as mean ± SE from three independent experiments. $^*P < 0.05$ as compared to that on 0 day (a) or with 0 mM (b).

https://doi.org/10.1371/journal.pone.0243859.g001

Contribution of GLUT isoforms to the growth of canine melanoma cells

We investigated the mRNA expression of GLUT isoforms in canine melanoma cells by RT-PCR. As shown in Fig 3A, the mRNA expression of *GLUT1* and *GLUT3*, but not that of *GLUT2* and *GLUT4*, was detected in canine melanoma cells. We observed that *GLUT1* and *GLUT3* mRNA dominantly expressed in additional canine melanoma cell lines (S6 Fig). The protein expression of GLUT1 and GLUT3 was also observed by western blotting (Fig 3B, scramble control).

To elucidate the contribution of GLUT1 and GLUT3 to the growth of canine melanoma cells, we examined the effect of the knockdown of GLUT1 and GLUT3 expression by siRNA transfection. The expression of GLUT1 and GLUT3 proteins decreased in the cells transfected with GLUT1 and GLUT3 siRNAs, respectively, but not that in those transfected with scrambled siRNA (Fig 3B–3D). The expression of β-actin used as an internal standard showed no alterations following transfection of cells with GLUT1, GLUT3, and scramble siRNAs (Fig 3B). The growth, glucose consumption, lactate secretion and glucose uptake of the cells transfected with GLUT1 and GLUT3 siRNAs were clearly attenuated (Fig 3E–3H). These results suggest that GLUT1 and GLUT3 play an important role in the growth of melanoma cells. Therefore, GLUT1 and GLUT3 may serve as promising targets for anticancer therapy of melanoma.

Discussion

In this study, we demonstrated that 2-DG induced inhibition of the growth of canine melanoma cells. 2-DG is a glycolytic inhibitor that is taken up by cells via GLUTs as well as glucose, and is subsequently phosphorylated by hexokinase to form 2-deoxy-D-glucose-6-phosphate (2-DG-6-P). 2-DG-6-P fails to undergo further metabolism via glycolysis but accumulates and inhibits hexokinase and phosphoglucose isomerase, which are involved in the first step of glucose metabolism [40–42]. The consequences involve downstream inhibition of glycolysis and induction of oxidative stress [1, 39]. Although this effect of 2-DG is known, 2-DG is thought to interfere with *N*-linked glycosylation of proteins [35], consequently leading to endoplasmic reticulum stress and apoptosis [36]. As the depletion of glucose can lead to cancer cell death via more than one mechanism, 2-DG is considered as a potent therapeutic agent against various cancer cells [36–39]. Therefore, our observations support the notion that the anti-glycolytic strategy via depletion of glucose is promising for canine melanoma treatment.

We also demonstrated that the GLUT inhibitor WZB-117 inhibited the growth of canine melanoma cells. This observation suggests that the inhibition of GLUTs results in the suppression of cell growth by reducing glycolysis because glucose is transported across the cell membrane via GLUT in a rate-limiting step [4–7]. In a previous study, the increase in the glucose uptake rate was observed during cellular alterations and conversion to malignancy in fibroblasts infected with sarcoma viruses [43]. Upregulation in glucose transport has been considered to be associated with the overexpression of GLUTs. In human melanoma cell lines such
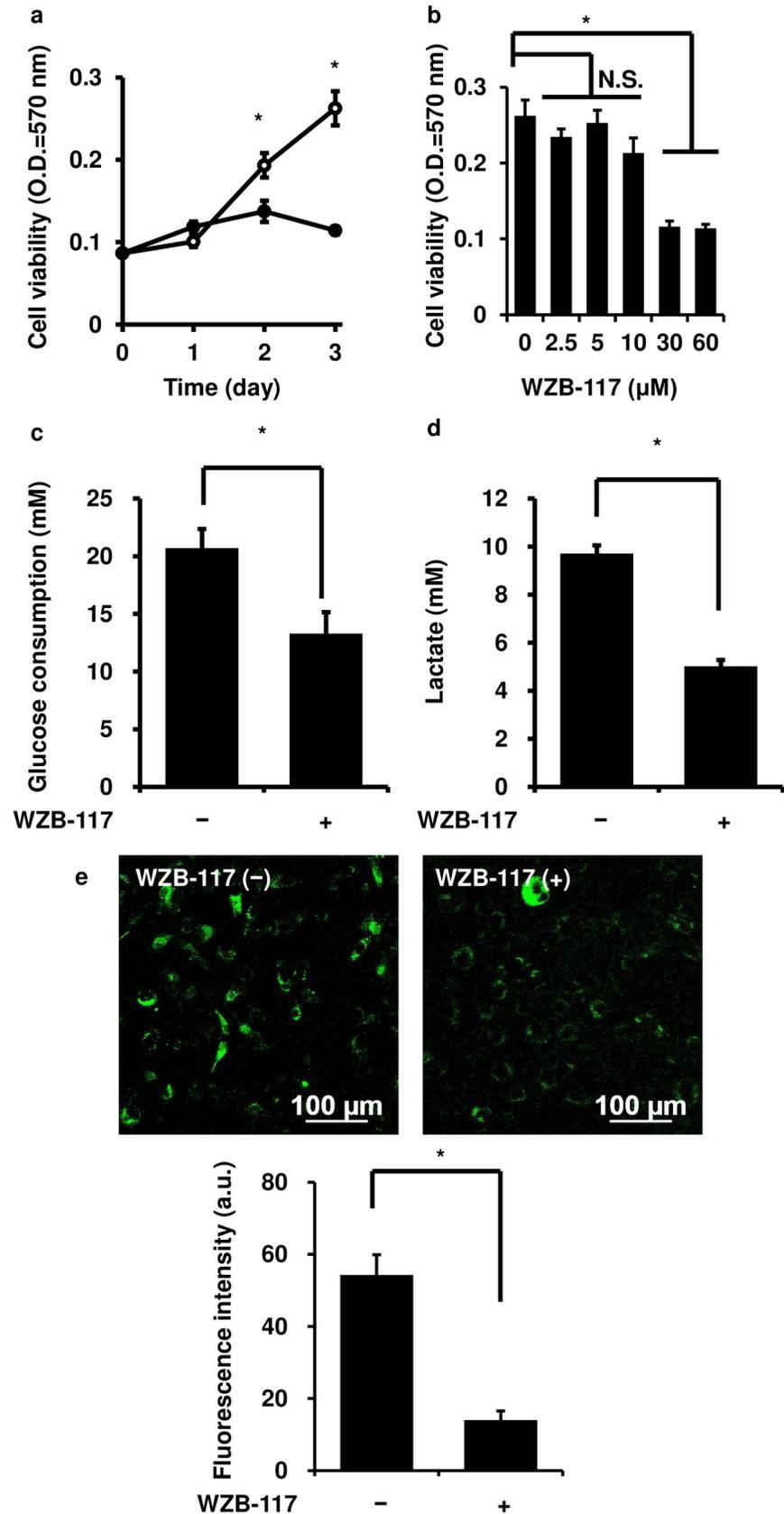
Fig 2. Effect of a GLUT inhibitor on the growth of canine melanoma cells. (a) Time-dependent changes in the growth of canine melanoma cells with (closed circle) or without (open circle) GLUT inhibitor WZB-117 treatment. The cells were incubated for 3 days with 60 μM WZB-117, which significantly attenuated their growth. (b) Dose-dependent effect of WZB-117 on the growth of canine melanoma cells. The cells were incubated with 0 to 60 μM WZB-117, which attenuated their growth in a dose-dependent manner. (c) The effect of WZB-117 on glucose consumption of canine melanoma cells. The cells were incubated with 60 μM WZB-117 for 3 days, and glucose consumption was found to be significantly attenuated. (d) The effect of WZB-117 on lactate secretion of canine melanoma cells. The cells were incubated with 60 μM WZB-117 for 3 days, and lactate secretion was found to be significantly attenuated. (e) The effect of WZB-117 on glucose uptake of canine melanoma cells. The cells were incubated with 60 μM WZB-117 for 3 days, and glucose uptake was found to be significantly attenuated. Results are shown as mean ± SE from three independent experiments. $^*P < 0.05$ as compared to that on 0 day (a) or with 0 μM (b).

as WM3211, Mel-Im and SbCl2, the dose-dependent reduction in glucose consumption and cell growth has been previously observed following treatment with a GLUT inhibitor [44]. Therefore, the inhibition of GLUTs could be exploited as an anticancer strategy for canine melanoma.

We found that canine melanoma cells expressed GLUT1 and GLUT3. GLUT1 and GLUT3 have high affinity (*K*m 3 and 1.4 mmol/L, respectively) for glucose that may contribute to optimization of the energy supply, thereby providing a fundamental advantage for the growth of cancer cells [45, 46]. In humans, the upregulation in the expression of GLUT1 and GLUT3 has been observed in the majority of cancers (e.g., lung, brain, breast, bladder, cervical, colorectal, esophageal, hepatocellular, ovarian, renal cell, pancreatic, and prostate cancers) and has been linked to poor survival and tumor aggressiveness [10, 47, 48]. In stage I non-small cell lung carcinoma [49], oral squamous cell carcinoma [50], breast carcinoma [51], thyroid carcinoma [52], and laryngeal carcinoma [53], the overexpression of both GLUT1 and GLUT3 genes and proteins has been reported to be associated with poor survival. Therefore, the deregulated expression of these GLUTs has been associated with malignancy [54]. Regarding human melanoma, GLUT1 and GLUT3 are expressed in malignant and benign melanocytic lesions [55]. However, GLUT1 expression was found to be downregulated in malignant melanoma in this study. On the other hand, GLUT1 and GLUT3 are considered as potentially useful markers for the differentiation of melanoma from nevi, as patients with GLUT1- and GLUT3-positive melanomas had significantly lower survival rate than those who lacked GLUT1 and GLUT3 expression in their melanomas [13, 56, 57]. Therefore, it is conceivable that the upregulation of GLUT1 and GLUT3 expression is related to the malignancy of melanoma as well as other cancers. However, the contribution of GLUT1 and GLUT3 to this biological phenomenon has been unclear in melanoma cells. The growth of GLUT1 siRNA-transfected mouse B16 melanoma cells was reduced [41]. We also demonstrated that the transfection with GLUT1 and GLUT3 siRNAs resulted in the attenuation of the growth of canine melanoma cells. The uptake of the glucose analogue 2-deoxy-2-[^{18}F]-fluoro-D-glucose is closely related to GLUT1 and GLUT3 expression in malignant melanoma [58]. Taken together, it is likely that both GLUT1 and GLUT3 contribute to the glucose transport necessary for the growth of melanoma cells.

Silencing of GLUT1 and GLUT3 expressions by siRNA transfection was shown to enhance the apoptosis of oral squamous cell carcinoma cells and acute myeloid leukemia cells, respectively [59, 60]. Therefore, siRNA interference against GLUT1 and GLUT3 appears to be a valuable tool for the gene therapy of canine melanoma. As GLUT1 has been reported to be ubiquitously distributed in all tissues [10] and GLUT3 is predominantly expressed in neuronal tissues, placenta, testis, myocardium, and platelets in humans [10, 61–63], GLUT3 appears to be a more promising therapeutic target for the specific treatment of melanoma.
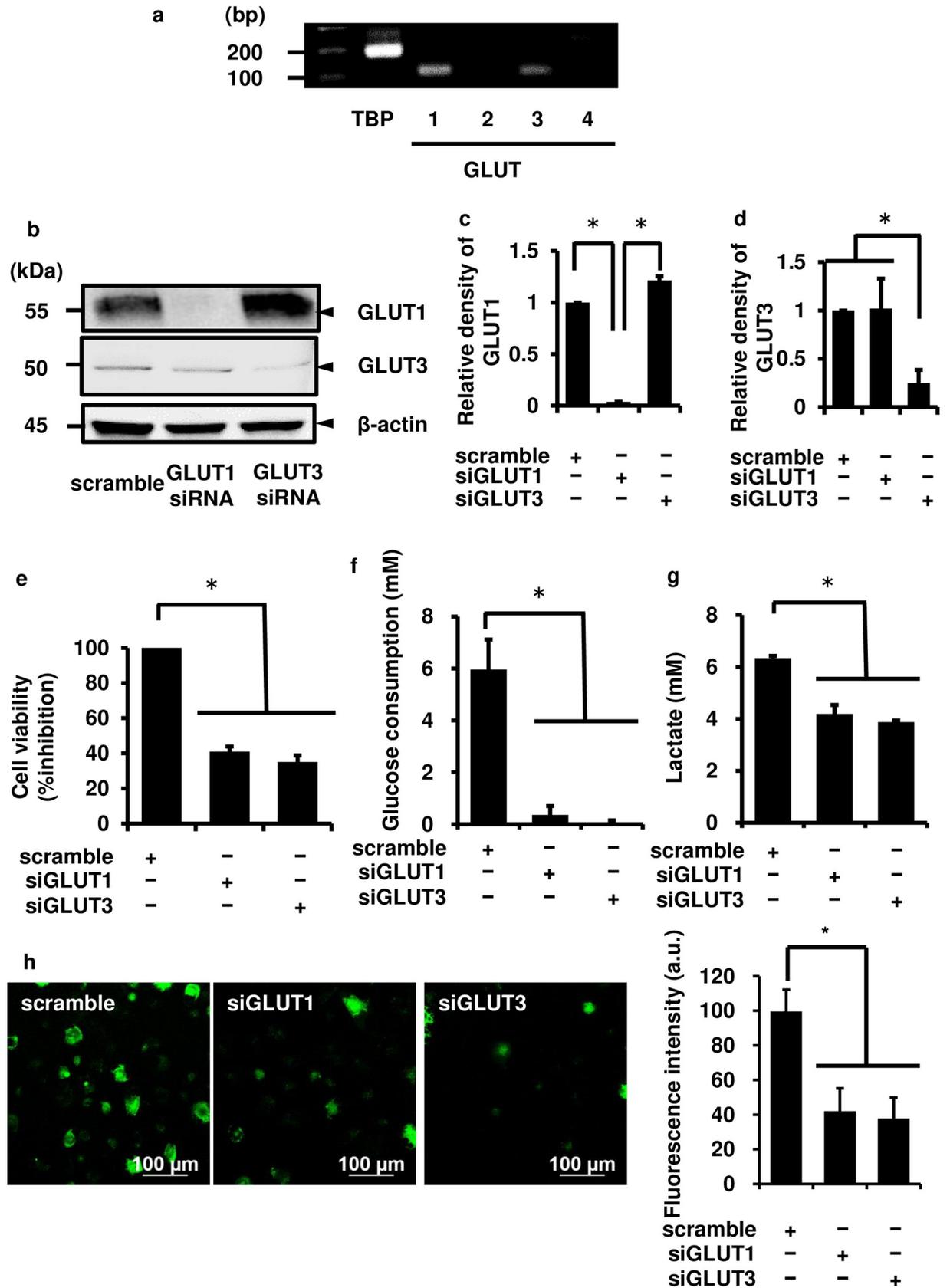
Fig 3. Contribution of GLUT isoforms to the growth of canine melanoma cells. (a) The mRNA expression of GLUT isoforms was detected by RT-PCR. The mRNA expression of *GLUT1* and *GLUT3*, but not *GLUT2* and *GLUT4*, was observed in canine melanoma cells. (b-d) The cells were transfected with GLUT1, GLUT3, and scrambled siRNAs and the expression of GLUT1, GLUT3, and β-actin was detected by western blotting. GLUT1 and GLUT3 siRNA transfection decreased the expression of GLUT1 and GLUT3, respectively, while scrambled siRNA transfection did not alter their expression. β-actin was used as an internal standard. Representative results (b) and relative density of GLUT1 or GLUT3 protein expression in siRNA-transfected cells as compared to those in scrambled siRNA-transfected cells (c, d) are shown. (e) The growth of canine melanoma cells was attenuated after 3 days of GLUT1 and GLUT3 siRNA transfection. (f) The glucose consumption of canine melanoma cells was attenuated after 3 days of GLUT1 and GLUT3 siRNA transfection. (g) The lactate secretion of canine melanoma cells was attenuated after 3 days of GLUT1 and GLUT3 siRNA transfection. (h) Glucose uptake was found to be significantly attenuated in the cells transfected with GLUT1 and GLUT3 siRNA. Results are presented as mean ± SE from three independent experiments. $^*P < 0.05$.

https://doi.org/10.1371/journal.pone.0243859.g003

Conclusion

As melanoma is less responsive to the existing therapeutic approach, our observations provide a new insight into the role of GLUT subtypes, GLUT1 and GLUT3, in cell growth and high-light an anti-glycolytic strategy as a promising tool for the treatment of canine melanoma.

Supporting information

S1 Fig. The effect of 2-DG on cell growth of several canine melanoma cell lines (KMeC and CMec-1). The cells were incubated with 5 mM 2-DG for 3 days, and cell growth was found to be significantly attenuated.
(PDF)

S2 Fig. The effect of 2-DG on glucose consumption and lactate secretion of several canine melanoma cell lines (KMeC and CMec-1). The cells were incubated with 5mM 2-DG for 3 days, and glucose and lactate secretion were found to be significantly attenuated.
(PDF)

S3 Fig. The effect of WZB-117 on cell growth of several canine melanoma cell lines (KMeC and CMec-1). The cells were incubated with 60μM WZB-117 for 3 days, and cell growth was found to be significantly attenuated.
(PDF)

S4 Fig. The effect of WZB-117 on glucose consumption and lactate secretion of several canine melanoma cell lines (KMeC and CMec-1). The cells were incubated with 60 μM WZB-117 for 3 days, and glucose consumption and lactate secretion were found to be significantly attenuated.
(PDF)

S5 Fig. The effect of WZB-117 on glucose consumption and lactate secretion of several canine melanoma cell lines (KMeC and CMec-1). The cells were incubated with 5 mM 2-DG or 60 μM WZB-117 for 24 h, and glucose uptake was found to be significantly attenuated.
(PDF)

S6 Fig. The MRNA expression of GLUT isoforms in canine melanoma cell lines.
(PDF)

S7 Fig. Uncropped images for the blots shown in Fig 3.
(PDF)

Acknowledgments

Author Contributions

References

1. Pelicano H, Martin DS, Xu RH, Huang P. Glycolysis inhibition for anticancer treatment. Oncogene 2006; 25: 4633–4646. https://doi.org/10.1038/sj.onc.1209597 PMID: 16892078

2. Koppenol WH, Bounds PL, Dang CV. Otto Warburg's contributions to current concepts of cancer metabolism. Nat Rev Cancer 2011; 11: 325–337. https://doi.org/10.1038/nrc3038 PMID: 21508971

3. Lu J, Tan M, Cai Q. The Warburg effect in tumor progression: mitochondrial oxidative metabolism as an anti-metastasis mechanism. Cancer Lett 2015; 356: 156–164. https://doi.org/10.1016/j.canlet.2014.04.001 PMID: 24732809

4. Uldry M, Thorens B. The SLC2 family of facilitated hexose and polyol transporters. Pflügers Arch 2004; 447: 480–489. https://doi.org/10.1007/s00424-003-1085-0 PMID: 12750891

5. Thorens B, Mueckler M. Glucose transporters in the 21st Century. Am J Physiol Endocrinol Metab 2010; 298: E141–E145. https://doi.org/10.1152/ajpendo.00712.2009 PMID: 20009031

6. Mueckler M, Thorens B. The SLC2 (GLUT) family of membrane transporters. Mol Aspects Med 2013; 34: 121–138. https://doi.org/10.1016/j.mam.2012.07.001 PMID: 23506862

7. Long W, Cheeseman CI. Structure of, and functional insight into the GLUT family of membrane transporters. Cell Health and Cytoskeleton 2015; 7: 167–183.

8. Calvo MB, Figueroa A, Pulido EG, Campelo RG, Aparicio LA. Potential role of sugar transporters in cancer and their relationship with anticancer therapy. Int J Endocrinol 2010; 2010. pii: 205357. https://doi.org/10.1155/2010/205357 PMID: 20706540

9. Adekola K, Rosen ST, Shanmugam M. Glucose transporters in cancer metabolism. Curr Opin Oncol 2012; 24: 650–654. https://doi.org/10.1097/CCO.0b013e328356da72 PMID: 22913968

10. Barron CC, Bilan PJ, Tsakiridis T, Tsiani E. Facilitative glucose transporters: Implications for cancer detection, prognosis and treatment. Metabolism 2016; 65: 124–139. https://doi.org/10.1016/j.metabol.2015.10.007 PMID: 26773935

11. Ancey PB, Contat C, Meylan E. Glucose transporters in cancer—from tumor cells to the tumor microenvironment. FEBS J 2018; 285: 2926–2943. https://doi.org/10.1111/febs.14577 PMID: 29893496

12. Parente P, Coli A, Massi G, Mangoni A, Fabrizi MM, Bigotti G. Immunohistochemical expression of the glucose transporters Glut-1 and Glut-3 in human malignant melanomas and benign melanocytic lesions. J Exp Clin Cancer Res 2008; 27: 34. https://doi.org/10.1186/1756-9966-27-34 PMID: 18764953

13. Důra M, Němejcová K, Jakša R, Bártů M, Kodet O, Tichá I, et al. Expression of Glut-1 in malignant melanoma and melanocytic nevi: an immunohistochemical study of 400 Cases. Pathol Oncol Res 2019; 25: 361–368. https://doi.org/10.1007/s12253-017-0363-7 PMID: 29128957

14. Bergman PJ. Canine oral melanoma. Clin Tech Small Anim Pract 2007; 22: 55–60. https://doi.org/10.1053/j.ctsap.2007.03.004 PMID: 17591290

15. Simpson RM, Bastian BC, Michael HT, Webster JD, Prasad ML, Conway CM, et al. Sporadic naturally occurring melanoma in dogs as a preclinical model for human melanoma. Pigment Cell Melanoma Res 2014; 27: 37–47. https://doi.org/10.1111/pcmr.12185 PMID: 24128326

16. Atherton MJ, Morris JS, McDermott MR, Lichty BD. Cancer immunology and canine malignant melanoma: A comparative review. Vet Immunol Immunopathol 2016; 169: 15–26. https://doi.org/10.1016/j.vetimm.2015.11.003 PMID: 26827834

17. Hernandez B, Adissu HA, Wei BR, Michael HT, Merlino G, Simpson RM. Naturally occurring canine melanoma as a predictive comparative oncology model for human mucosal and other triple wild-type melanomas. Int J Mol Sci 2018; 19. pii: E394. https://doi.org/10.3390/ijms19020394 PMID: 29385676

18. Inoue K, Ohashi E, Kadosawa T, Hong SH, Matsunaga S, Mochizuki M, et al. Establishment and characterization of four canine melanoma cell lines. J Vet Med Sci. 2004; 66: 1437–40. https://doi.org/10.1292/jvms.66.1437 PMID: 15585963

19. Endo Y, Watanabe M, Miyajima-Magara N, Igarashi M, Mochizuki M, Nishimura R, et al. DNA aneuploidy and centrosome amplification in canine tumor cell lines. Tissue and Cells. 2019; 61: 67–71. https://doi.org/10.1016/j.tice.2019.09.003 PMID: 31759409

20. Yoshitake R., Saeki K., Watanabe M., Nakaoka N., Ong S.M., Hanafusa M., et al. Molecular investigation of the direct anti-tumour effects of nonsteroidal anti-inflammatory drugs in a panel of canine cancer cell lines. Vet J. 2017; 221: 38–47. https://doi.org/10.1016/j.tvjl.2017.02.001 PMID: 28283079

21. Kitanaka N, Nakano R, Kitanaka T, Namba S, Konno T, Nakayama T, et al. NF-κB p65 and p105 implicate in interleukin 1β-mediated COX-2 expression in melanoma cells. PLoS One 2018; 13: e0208955. https://doi.org/10.1371/journal.pone.0208955 PMID: 30562372

22. Nakano R, Edamura K, Nakayama T, Narita T, Okabayashi K, Sugiya H. Fibroblast Growth Factor Receptor-2 Contributes to the Basic Fibroblast Growth Factor-Induced Neuronal Differentiation in Canine Bone Marrow Stromal Cells via Phosphoinositide 3-Kinase/Akt Signaling Pathway. PLoS One 2015; 10: e0141581. https://doi.org/10.1371/journal.pone.0141581 PMID: 26523832

23. Nakano R, Edamura K, Sugiya H, Narita T, Okabayashi K, Moritomo T, et al. Evaluation of mRNA expression levels and electrophysiological function of neuron-like cells derived from canine bone marrow stromal cells, Am J Vet Res 2013; 74: 1311–1320. https://doi.org/10.2460/ajvr.74.10.1311 PMID: 24066915

24. Tsuchiya H, Nakano R, Konno T, Okabayashi K, Narita T, Sugiya H. Activation of MEK/ERK pathways through NF-κB activation is involved in interleukin-1β-induced cyclooxygenease-2 expression in canine dermal fibroblasts. Vet Immunol Immunopathol 2015; 168: 223–232. https://doi.org/10.1016/j.vetimm.2015.10.003 PMID: 26549149

25. Nakano R, Edamura K, Nakayama T, Teshima K, Asano K, Narita T, et al. Differentiation of canine bone marrow stromal cells into voltage- and glutamate-responsive neuron-like cells by basic fibroblast growth factor. J Vet Med Sci 2015; 77: 27–35. https://doi.org/10.1292/jvms.14-0284 PMID: 25284120

26. Konno T, Nakano R, Mamiya R, Tsuchiya H, Kitanaka T, Namba S, et al. Expression and function of interleukin-1β-induced neutrophil gelatinase-associated lipocalin in renal tubular cells, PLOS ONE 2016; 11: e0166707. https://doi.org/10.1371/journal.pone.0166707 PMID: 27851800

27. Kitanaka T, Nakano R, Kitanaka N, Kimura T, Okabayashi K, Narita T, et al. JNK activation is essential for activation of MEK/ERK signaling in IL-1β-induced COX-2 expression in synovial fibroblasts. Sci Rep 2017; 7: 39914. https://doi.org/10.1038/srep39914 PMID: 28054591

28. Namba S, Nakano R, Kitanaka T, Kitanaka N, Nakayama T, Sugiya H. ERK2 and JNK1 contribute to TNF-α-induced IL-8 expression in synovial fibroblasts. PLoS One 2017; 12: e0182923. https://doi.org/10.1371/journal.pone.0182923 PMID: 28806729

29. Kitanaka N, Nakano R, Sugiura K, Kitanaka T, Namba S, Konno T, et al. Interleukin-1β promotes interleulin-6 expression via ERK1/2 signaling pathway in canine dermal fibroblasts. PLOS ONE 2019; 14: e0220262. https://doi.org/10.1371/journal.pone.0220262 PMID: 31344106

30. Kitanaka N, Nakano R, Sakai M, Kitanaka T, Namba S, Konno T, et al. ERK1/ATF-2 signaling axis contributes to interleukin-1β-induced MMP-3 expression in dermal fibroblasts. PLOS ONE 2019; 14: e0222869. https://doi.org/10.1371/journal.pone.0222869 PMID: 31536594

31. Nakano R, Kitanaka T, Namba S, Kitanaka N, Sugiya H. Protein kinase Cε regulates nuclear translocation of extracellular signal-regulated kinase, which contributes to bradykinin-induced cyclooxygenase-2 expression. Sci Rep 2018; 8: 8535. https://doi.org/10.1038/s41598-018-26473-7 PMID: 29867151

32. Nakano R, Kitanaka T, Namba S, Kitanaka N, Sato M, Shibukawa Y, et al. All-trans retinoic acid induces reprogramming of canine dedifferentiated cells into neuron-like cells. PLoS One 2020; 15: e0229892. https://doi.org/10.1371/journal.pone.0229892 PMID: 32231396

33. Bradford MM. A rapid and sensitive method for the quantitation of microgram quantities of protein utilizing the principle of protein-dye binding. Anal Biochem 1976; 72: 248–254. https://doi.org/10.1006/abio.1976.9999 PMID: 942051

34. Bertoni JM. Competitive inhibition of rat brain hexokinase by 2-deoxyglucose, glucosamine, and metrizamide. J Neurochem 1981; 37: 1523–1528. https://doi.org/10.1111/j.1471-4159.1981.tb06322.x PMID: 7334375

35. Kurtoglu M, Gao N, Shang J, Maher JC, Lehrman MA, Wangpaichitr M, et al. Under normoxia, 2-deoxy-D-glucose elicits cell death in select tumor types not by inhibition of glycolysis but by interfering with N-linked glycosylation. Mol Cancer Ther 2007; 6: 3049–3058. https://doi.org/10.1158/1535-7163.MCT-07-0310 PMID: 18025288

36. Kurtoglu M, Maher JC, Lampidis TJ. Differential toxic mechanisms of 2-deoxy-D-glucose versus 2-fluorodeoxy-D-glucose in hypoxic and normoxic tumor cells. Antioxid Redox Signal 2007; 9: 1383–1390. https://doi.org/10.1089/ars.2007.1714 PMID: 17627467

37. Ralser M, Wamelink MM, Struys EA, Joppich C, Krobitsch S, Jakobs C, et al. A catabolic block does not sufficiently explain how 2-deoxy-D-glucose inhibits cell growth. Proc Natl Acad Sci U S A 2008; 105: 17807–17811. https://doi.org/10.1073/pnas.0803090105 PMID: 19004802

38. Giammarioli AM, Gambardella L, Barbati C, Pietraforte D, Tinari A, Alberton M, et al. Differential effects of the glycolysis inhibitor 2-deoxy-D-glucose on the activity of pro-apoptotic agents in metastatic melanoma cells, and induction of a cytoprotective autophagic response. Int J Cance 2012; 131: E337–E347.29.

39. Zhang D, Li J, Wang F, Hu J, Wang S, Sun Y. 2-Deoxy-D-glucose targeting of glucose metabolism in cancer cells as a potential therapy. Cancer Lett 2014; 355: 176–183. https://doi.org/10.1016/j.canlet.2014.09.003 PMID: 25218591

40. Wick AN, Drury DR, Nakada HI, Wolfe JB. Localization of the primary metabolic block produced by 2-deoxyglucose. J Biol Chem 1957; 224: 963–969. PMID: 13405925

41. Chen W, Guéron M. The inhibition of bovine heart hexokinase by 2-deoxy-D-glucose-6-phosphate: characterization by ^{31}P NMR and metabolic implications. Biochimie 1992; 74: 867–873. https://doi.org/10.1016/0300-9084(92)90070-u PMID: 1467345

42. Spitz DR, Sim JE, Ridnour LA, Galoforo SS, Lee YJ. Glucose deprivation-induced oxidative stress in human tumor cells. A fundamental defect in metabolism? Ann N Y Acad Sci 2000; 899: 349–362. https://doi.org/10.1111/j.1749-6632.2000.tb06199.x PMID: 10863552

43. Hatanaka M. Transport of sugars in tumor cell membranes. Biochim Biophys Acta 1974; 355: 77–104. https://doi.org/10.1016/0304-419x(74)90008-0 PMID: 4371599

44. Koch A, Lang SA, Wild PJ, Gantner S, Mahli A, Spanier G, et al. Glucose transporter isoform 1 expression enhances metastasis of malignant melanoma cells. Oncotarget 2015; 6: 32748–32760. https://doi.org/10.18632/oncotarget.4977 PMID: 26293674

45. Colville CA, Seatter MJ, Jess TJ, Gould GW, Thomas HM. Kinetic analysis of the liver-type (GLUT2) and brain-type (GLUT3) glucose transporters in Xenopus oocytes: substrate specificities and effects of transport inhibitors. Biochem J 1993; 290: 701–706. https://doi.org/10.1042/bj2900701 PMID: 8457197

46. Uldry M, Ibberson M, Hosokawa M, Thorens B. GLUT2 is a high affinity glucosamine transporter. FEBS Lett 2002; 524: 199–203. https://doi.org/10.1016/s0014-5793(02)03058-2 PMID: 12135767

47. Yamamoto T, Seino Y, Fukumoto H, Koh G, Yano H, Inagaki N, et al. Over-expression of facilitative glucose transporter genes in human cancer. Biochem Biophys Res Commun 1990; 170: 223–230. https://doi.org/10.1016/0006-291x(90)91263-r PMID: 2372287

48. Younes M, Lechago LV, Somoano JR, Mosharaf M, Lechago J. Wide expression of the human erythrocyte glucose transporter Glut1 in human cancers. Cancer Res 1996; 56: 1164–1167. PMID: 8640778

49. Younes M, Brown RW, Stephenson M, Gondo M, Cagle PT. Overexpression of Glut1 and Glut3 in stage I nonsmall cell lung carcinoma is associated with poor survival. Cancer 1997; 80: 1046–1051. https://doi.org/10.1002/(sici)1097-0142(19970915)80:6<1046::aid-cncr6>3.0.co;2-7 PMID: 9305704

50. Ayala FR, Rocha RM, Carvalho KC, Carvalho AL, da Cunha IW, Lourenço SV, et al. GLUT1 and GLUT3 as potential prognostic markers for Oral Squamous Cell Carcinoma. Molecules 2010; 15: 2374–2387. https://doi.org/10.3390/molecules15042374 PMID: 20428049

51. Krzeslak A, Wojcik-Krowiranda K, Forma E, Jozwiak P, Romanowicz H, Bienkiewicz A, et al. Expression of GLUT1 and GLUT3 glucose transporters in endometrial and breast cancers. Pathol Oncol Res 2012; 18: 721–728. https://doi.org/10.1007/s12253-012-9500-5 PMID: 22270867

52. Jóźwiak P, Krześlak A, Pomorski L, Lipińska A. Expression of hypoxia-related glucose transporters GLUT1 and GLUT3 in benign, malignant and non-neoplastic thyroid lesions. Mol Med Rep 2012; 6: 601–606. https://doi.org/10.3892/mmr.2012.969 PMID: 22752218

53. Starska K, Forma E, Jóźwiak P, Bryś M, Lewy-Trenda I, Brzezińska-Błaszczyk E, et al. Gene and protein expression of glucose transporter 1 and glucose transporter 3 in human laryngeal cancer-the relationship with regulatory hypoxia-inducible factor-1α expression, tumor invasiveness, and patient prognosis. Tumour Biol 2015; 36: 2309–2321. https://doi.org/10.1007/s13277-014-2838-4 PMID: 25412955

54. Chen X, Lu P, Zhou S, Zhang L, Zhao JH, Tang JH. Predictive value of glucose transporter-1 and glucose transporter-3 for survival of cancer patients: A meta-analysis. Oncotarget 2017; 8: 13206–13213. https://doi.org/10.18632/oncotarget.14570 PMID: 28086215

55. Parente P, Coli A, Massi G, Mangoni A, Fabrizi MM, Bigotti G. Immunohistochemical expression of the glucose transporters Glut-1 and Glut-3 in human malignant melanomas and benign melanocytic lesions. J Exp Clin Cancer Res 2008; 27: 34. https://doi.org/10.1186/1756-9966-27-34 PMID: 18764953

56. Yan S, Coffing BN, Li Z, Xie H, Brennick JB, Beg HA, et al. Diagnostic and prognostic value of ProEx C and GLUT1 in melanocytic lesions. Anticancer Res 2016; 36: 2871–2880. PMID: 27272799

57. Ruby KN, Liu CL, Li Z, Felty CC, Wells WA, Yan S. Diagnostic and prognostic value of glucose transporters in melanocytic lesions. Melanoma Res 2019; 29: 603–611. https://doi.org/10.1097/CMR.0000000000000626 PMID: 31135601

58. Park SG, Lee JH, Lee WA, Han KM. Biologic correlation between glucose transporters, hexokinase-II, Ki-67 and FDG uptake in malignant melanoma. Nucl Med Biol 2012; 39: 1167–1172. https://doi.org/10.1016/j.nucmedbio.2012.07.003 PMID: 22901702

59. Shimanishi M, Ogi K, Sogabe Y, Kaneko T, Dehari H, Miyazaki A, et al. Silencing of GLUT-1 inhibits sensitization of oral cancer cells to cisplatin during hypoxia. J Oral Pathol Med 2013; 42: 382–388. https://doi.org/10.1111/jop.12028 PMID: 23227892

60. Zhuang Y, Zhao J, Xu X, Bi L. Downregulation of GLUT3 promotes apoptosis and chemosensitivity of acute myeloid leukemia cells via EGFR signaling. Arch Iran Med 2018; 21: 73–78. PMID: 29664658

61. Bell GI, Burant CF, Takeda J, Gould GW. Structure and function of mammalian facilitative sugar transporters. J Biol Chem 1993; 268: 19161–19164. PMID: 8366068

62. Craik JD, Stewart M, Cheeseman CI. GLUT-3 (brain-type) glucose transporter polypeptides in human blood platelets. Thromb Res 1995; 79: 461–469. https://doi.org/10.1016/0049-3848(95)00136-f PMID: 7502272

63. Grover-McKay M, Walsh SA, Thompson SA. Glucose transporter 3 (GLUT3) protein is present in human myocardium. Biochim Biophys Acta 1999; 1416: 145–154. https://doi.org/10.1016/s0005-2736(98)00216-8 PMID: 9889355